POLITECNICO DI TORINO
Repository ISTITUZIONALE

Energy Savings Assessment on a Mid-Size Excavator with Common Pressure Rail Architecture

Original
Energy Savings Assessment on a Mid-Size Excavator with Common Pressure Rail Architecture / Rundo, M., Misul, D.A., Miretti, F., Gargiani, G., Magnati, A., Moffa, G., Conte, C.. - In: JOURNAL OF PHYSICS. CONFERENCE SERIES. - ISSN 1742-6588. - ELETTRONICO. - 3143:(2025), pp. 1-15. (80° Congresso Nazionale ATI Benevento 10-12 settembre 2025) [10.1088/1742-6596/3143/1/012064].

Availability:
This version is available at: 11583/3005703 since: 2025-12-07T08:43:48Z

Publisher:
IOP Publishing

Published
DOI:10.1088/1742-6596/3143/1/012064

Terms of use:

This article is made available under terms and conditions as specified in the corresponding bibliographic description in the repository

Publisher copyright

(Article begins on next page)

19 November 2026

Journal of Physics:
Conference Series

PURPOSE-LED PUBLISHING™

PAPER • **OPEN ACCESS**

Energy Savings Assessment on a Mid-Size Excavator with Common Pressure Rail Architecture

To cite this article: Massimo Rundo *et al* 2025 *J. Phys.: Conf. Ser.* **3143** 012064

View the article online for updates and enhancements.

You may also like

- Development and Validation of a Mini Excavator Model: A Numerical Tool for Hydraulic and Control System Design
Andrea Fornaciari, Alice Betti, Barbara Zardin et al.
- EnerCmed Project: Advancing Energy-Positive and Climate-Resilient Hinterlands through Renewable Energy Communities and Nature-Based Solutions
Jonathan Roberts, Augusto Bocanegra, Davide Borelli et al.
- The Effect of Steam-Oxygen Gasifying Medium on Syngas Upgrading for Nitrogen Reduction
Marco Puglia, Bear Kaufmann, Jim Mason et al.



This content was downloaded from IP address 130.192.21.76 on 06/12/2025 at 09:09

Journal of Physics: Conference Series **3143** (2025) 012064 doi:10.1088/1742-6596/3143/1/012064

Energy Savings Assessment on a Mid-Size Excavator with Common Pressure Rail Architecture

Massimo Rundo[1*], Daniela Anna Misul[1], Federico Miretti[1], Giulia Gargiani[1], Alessio Magnati[1], Gabriele Moffa[1] and Carmine Conte[1]

[1] Department of Energy, Politecnico di Torino, Turin, Italy

[*]E-mail: massimo.rundo@polito.it

Abstract. In earthmoving machines, the prime mover transmits power to all actuators through hydraulic circuits. However, the use of flow control valves, which rely on pressure drops, leads to significant energy dissipation and fuel consumption. The shift toward electric propulsion, already in progress for mini excavators and expected to expand to larger machines, requires a sharp reduction in pump energy demand to match the operating range of diesel-powered vehicles.

This study simulates the performance of a recently proposed hydraulic architecture, based on a validated model of a mid-size excavator. Instead of imposing flow to the actuators via proportional directional control valves, the proposed system uses two-position valves to independently connect each actuator to two constant-pressure lines maintained by hydraulic accumulators. A proportional valve is retained for fine speed control but operates with lower pressure drops, thereby improving overall system efficiency.

The developed lumped parameter model preserves the original actuators and kinematics. Simulations reproduce dig-and-dump and levelling cycles, comparing fuel consumption against a Load Sensing system. Additional simulations reduce engine speed to increase efficiency, enabled by the greater flexibility in engine operation. Results show the proposed system can reduce fuel consumption by over 50%, demonstrating strong potential for enhancing excavator energy efficiency.

1. Introduction

Earthmoving machinery relies heavily on hydraulic systems to transfer power from the engine to the actuators, particularly for operations involving the boom, arm, bucket, and cabin rotation. These systems are favoured for their robustness, high power density, and precise control capabilities. However, conventional hydraulic architectures typically rely on proportional directional control valves that regulate actuator speed by throttling flow, which inherently causes pressure drops. As a result, a significant portion of the energy provided by the prime mover is dissipated as heat within the hydraulic circuit. In machines with heavy duty cycles, such as excavators, this inefficiency leads to considerable fuel consumption, especially during repetitive digging and loading operations, where multiple actuators are often engaged simultaneously


Content from this work may be used under the terms of the Creative Commons Attribution 4.0 licence. Any further distribution of this work must maintain attribution to the author(s) and the title of the work, journal citation and DOI.
Published under licence by IOP Publishing Ltd

under varying load conditions. These considerations highlight the urgent need to improve the energy efficiency of hydraulic systems in earthmoving equipment.

Load Sensing (LS) systems have long been a cornerstone of hydraulic circuit design in earthmoving machinery, offering improved energy efficiency by adapting the pump flow to the actual demand of the actuators. However, recent advancements have aimed at further reducing energy losses and enhancing system efficiency. Casoli et al. [1] analysed energy losses in the hydraulic circuit of a medium-sized agricultural tractor and proposed a load-sensing signal conditioner to reduce valve pressure drops. Similarly, Bonavolontà et al. [2] explored strategies to optimize LS systems in excavators, highlighting flow-sharing, pre- and post-compensated valves, and flow-on-demand control. They also introduced a hydraulic hybrid excavator with an Energy Recovery System, achieving up to 11% fuel savings during trench-digging cycles. Fassbender et al. [3] explored two alternative LS system architectures, comparing them to electrified valve-controlled LS systems across three machine types. One architecture employed a conventional LS system enhanced with an electric generator and hydraulic motor for flow metering, load compensation, and energy recovery, while the other integrated an electric motor driving the LS pump for low-energy functions and a variable-displacement pump for high-energy functions. In a 17-ton excavator, the latter architecture achieved a maximum energy saving of 48%, outperforming the former by 11%. Lastly, Tian et al. [4] investigated two approaches in the context of a tractor with a planter system. Their Hydraulic Load-Sensing solution retained the benefits of load sensing but affected dynamic performance, while the Intelligent Pressure Saturation Control actively adjusted the pump pressure, achieving a 38% improvement in efficiency.

As the industry moves towards electrification, especially with mini excavators, there is an increasing need to reduce the energy demand of hydraulic pumps to make electric propulsion competitive with diesel-powered systems. While electric drives offer advantages in terms of zero on-site emissions and control flexibility, their widespread adoption in larger earthmoving machines is hindered by the limited energy density of batteries, as well as the high continuous power demand of traditional hydraulic circuits. Consequently, improving the efficiency of hydraulic actuation becomes a key enabler for extending electric solutions to medium and large excavators without compromising performance or operating time.

In recent years, several studies have investigated alternative architectures aimed at improving the energy efficiency of hydraulic circuits in excavators. Among these, decentralized systems, where actuators are driven by local hydraulic units rather than a centralized valve block, have shown significant potential. Casoli et al. [5] evaluated Direct Driven Hydraulics on a 9-ton excavator by comparing cabin-mounted and actuator-mounted pump configurations. While reducing mechanical energy needs by removing traditional valves and pressure compensators, fuel savings were limited due to engine downsizing and friction losses in longer hydraulic lines. Fresia et al. [6] introduced a novel excavator architecture that reduces the required electric motor size by shifting most power transmission from electric to hydraulic. Using speed-controlled pumps connected to a centralized rail, the system incorporates realistic digging forces and cabin inertia. Simulations across six JCMAS-standard digging scenarios demonstrated its ability to manage varying loads, recover energy through supercapacitors, and perform under extreme conditions.

Building on this, advancements in electrification architectures for excavators aim to enhance vehicle efficiency, reduce emissions, and enable component downsizing. Schmidt et al. [7] proposed a hybrid electro-hydraulic/mechanical drive network (EDN) for excavator actuation,

reducing control volumes from six to four by short-circuiting cylinder chambers. The EDN achieved similar energy efficiency with less motor power, reduced power consumption by nearly 60%, increased total efficiency from 22% to 55%, and reduced tank volume by over 80% compared to traditional systems. In addition to architectural developments, recent research has also focused on optimizing control and eliminating unnecessary physical components in electro-hydraulic systems. Padovani [8] explored using observed pressure to introduce artificial damping in electro-hydraulic drives, replacing physical pressure transducers with a virtual sensor. A closed-loop position control system, based on a linearized model and a full-state Luenberger observer, accurately estimated actuator position and pressure differentials.

Digital hydraulics has emerged as a promising solution to overcome the limitations of conventional hydraulic systems. Zhang et al. [9] identified parallel digital hydraulic technology as a prominent research direction due to its inherent fault tolerance and fast dynamic response. However, the approach introduces challenges, including increased cost, larger system volume, and the lack of accurate, application-ready control algorithms, factors that currently limit its broader adoption. Sciatti et al. [10] highlight the energy inefficiencies of conventional hydraulic systems using analogue spool valves, which cause significant power losses. Despite their precision, these systems suffer from pressure drops across control components. Digital hydraulic technology offers a promising alternative by replacing spool valves with low-cost on/off valves. This shift aims to enhance energy efficiency and maintain hydraulic relevance in modern applications.

To address the increasing demand for energy-efficient solutions in the context of excavator electrification, this study investigates a recently proposed hydraulic architecture based on a common pressure rail concept. The proposed architecture replaces conventional proportional directional control valves with two-port two-position on/off valves that connect each actuator to one of two constant-pressure lines, maintained by hydraulic accumulators. For precise speed regulation, a proportional valve is still employed; however, it operates under much lower pressure drops, contributing to a notable improvement in overall system efficiency. Simulations, conducted on a validated mid-size excavator model, assess the fuel consumption under different duty cycles and compare the results with those from a traditional LS system. The outcomes highlight the potential of this architecture to significantly reduce energy demand, thereby supporting the transition to more sustainable construction machinery.

The paper is organized as follows. Section 2 describes the reference excavator, its hydraulic architecture, and the validation of the simulation model. Section 3 introduces the proposed system based on common pressure rails, detailing the circuit layout, modelling approach and control logic. Section 4 outlines the working cycles used for the analysis, specifically the dig-and-dump and levelling operations. In Section 5, simulation results are presented, including comparison in terms of actuator displacement, energy and fuel consumption between the reference and proposed systems, and an evaluation of engine downsizing effects. Finally, Section 6 summarizes the main findings and conclusions.

2. Reference hydraulic excavator

2.1 Machine description

This study focuses on a 9-ton excavator powered by a diesel engine with a peak output power of 50 kW. The machine hydraulic system follows a load-sensing principle with flow sharing. While the original configuration manages nine hydraulic functions, this analysis concentrates on four key operations: boom, arm, bucket, and swing. A simplified hydraulic schematic is provided in Fig. 1, excluding unused modules for clarity.

The hydraulic circuit is supplied by two pumps driven by the internal combustion engine. The first, a variable displacement axial piston pump (PU1), is equipped with torque and differential pressure limiter controls. The second, a gear pump (PU2), is dedicated to supplying the blade actuator and the swing motor. Both pumps are connected to a stack of proportional directional control valves.

The inlet module is linked to the delivery port of pump PU1 and incorporates the relief valve (RV1) to limit maximum pressure, as well as the unloading valve (UV) for discharging flow during standby conditions. Pump PU2 is directly connected to the blade module, where the relief valve (RV2) is located. Additionally, this pump supplies the hydraulic swing motor, which features an integrated holding brake.

Within the swing module, the boost valve (VB) enhances boom velocity when the hydraulic motor is also active. The boom, arm, and bucket modules are equipped with local compensators that maintain a constant pressure drop across the main spool, ensuring that actuator speed depends solely on the operator valve command.

An overcentre valve is installed on the boom and blade actuators, while anti-shock valves are present in both the outlet module (RV3) and the swing motor.

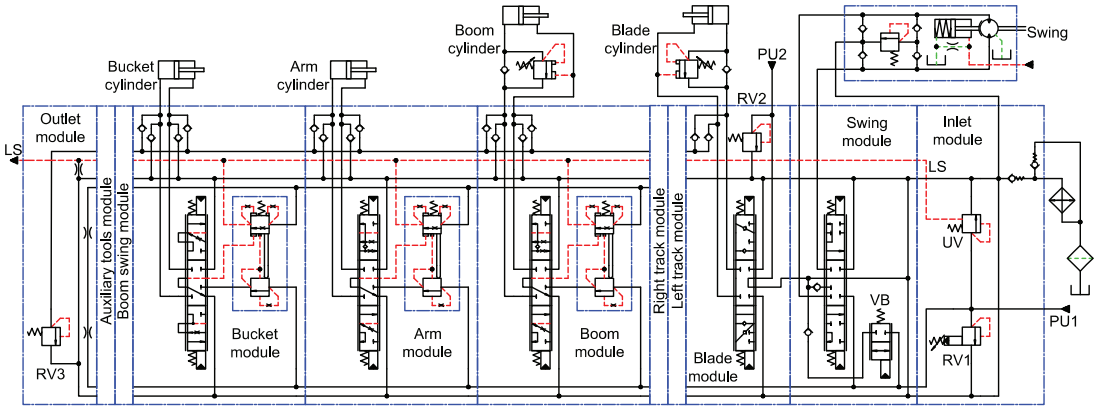


Figure 1. Simplified scheme of the original hydraulic circuit.

2.2 Simulation model and validation

Simulations have been carried out in the Simcenter Amesim® environment. The model used in this study is an updated version of a previous model developed by the authors [6]. In the updated reference model, the engine is modelled with an ideal prime mover to simplify the analysis process and focus on the hydraulic system. This approach also enhances accuracy, particularly at zero torque, while reducing simulation time during fuel consumption evaluation of the reference machine. The fuel consumption analysis relies on look-up tables derived from units used in similar applications. Given engine load torque and shaft speed as inputs, the table interpolates the corresponding fuel flow rate. The data used in the look-up table, shown in Fig.2, are derived from experimental measurements on a 6-cylinder turbocharged diesel engine with a 2.9-liter displacement. Since the same engine model is applied to both architectures under investigation, the comparison between the two layouts remains representative and consistent.

The engine speed is not directly controlled; instead, it is maintained at a high idle of 2400 rpm, with a variation of ±100 rpm throughout the tested cycles. Furthermore, within this range, the shaft speed is assumed to vary linearly with the load torque.

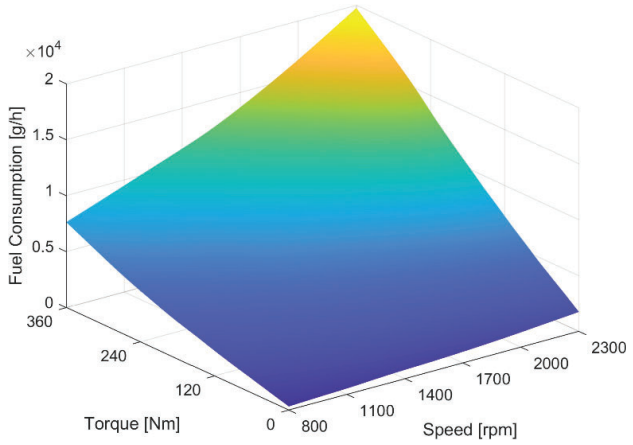


Figure 2. Fuel consumption map.

Additionally, the simulation model includes a comprehensive characterization of the various components within both the hydraulic and mechanical domains. Further details on the flow generation unit, the directional control valve stack, the actuators associated with the different functions, and the mechanical model (including arm kinematics, soil interaction during the digging phase, and cabin inertia variation with arm position) can be found in [6].

The reference excavator model was validated through experimental tests, where maximum positive and negative commands were applied to the directional control valves to assess actuator performance. The results for the arm and boom actuators confirm the model reliability, with simulated delivery pressure and flow rate closely matching experimental data. Key measurements included pump delivery pressure, flow rate, and engine speed, demonstrating accurate system behavior under varying load conditions. This validation ensures the model suitability for energy consumption analysis. More details on the experimental campaign can be found in the previous papers [6],[11].

3. Common Pressure Rail architecture

The Common Pressure Rail (CPR) system is an innovative advancement in hydraulic systems, enhancing energy efficiency and minimizing throttling losses. This approach enables the downsizing of both the pump and diesel engine [12], [13].

In traditional Load Sensing (LS) systems, throttling losses arise because the supply pressure must match the highest load pressure. This constant pressure differential between the pump and actuators results in substantial power losses, particularly when multiple actuators with varying pressure demands operate simultaneously. The CPR addresses these inefficiencies by introducing multiple pressure sources, ensuring actuators receive precise pressure levels tailored to their load requirements, thereby minimizing throttling losses. Two pressure rails, high pressure (HP) and medium pressure (MP), along with a low-pressure tank and accumulators, manage peak power demands and facilitate efficient engine operation at lower speeds. To further mitigate throttling losses when supplying flow to linear actuators, a series of on/off valves selectively connects both pressure rails and the tank line to the piston and rod chambers of each cylinder. This setup creates a system of nine artificial supply pressures, dynamically adjusting to load conditions to reduce throttling losses and enable energy recovery. A key advantage of this system is the optimized efficiency of engine and pump operation. Since these components solely charge the accumulators,

they are decoupled from immediate actuator power demands and function in a digital mode. When the accumulator state of charge drops, the engine and pump operate at full capacity until fully charged, at which point they idle, avoiding part-load inefficiencies and significantly reducing energy losses. Additionally, this architecture enhances the recovery of potential energy from the boom. By connecting the boom piston chamber to one of the two pressure rails, energy from lowering the actuator is stored in accumulators and can be redistributed to power other actuators. The system also prevents pressure peaks at actuator end-stops, a common issue in flow-controlled systems like LS. A constant pressure system mitigates this by supplying pressure rather than flow to the actuator.

3.1 Hydraulic circuit

The layout of the CPR circuit is illustrated in Fig. 3. The internal combustion engine (ICE) drives a variable displacement pump (HU), with its maximum outlet pressure limited by the relief valve RV3. The pump has a volumetric displacement of 75 cc/rev. A three-port three-position directional control valve (DV) manages the flow direction toward either the HP or the MP line, based on the accumulator charging strategy outlined in the control logic section.

The power supply system includes two accumulators (ACC1 and ACC2), which are used to maintain specific pressure levels within the respective hydraulic lines. To ensure system safety and pressure control, two relief valves (RV1 and RV2) are installed to limit pressure in the HP and MP lines. Additionally, two check valves (CV1 and CV2) are incorporated to prevent backflow to the pump, ensuring unidirectional flow and protecting system components.

The three common pressure lines supply hydraulic energy in parallel to the boom, arm, bucket, and swing modules. These modules consist of six on/off bidirectional valves and a four-port two-position proportional valve. The on/off valves are actuated to achieve the necessary pressure in the actuator chambers to counter the external forces acting on the rods. The proportional valve is modulated based on joystick commands from the operator, enabling precise control of actuator speed.

The actuator configuration remains consistent with the baseline LS system. The boom, arm, and bucket functions are actuated by single-rod, double-acting hydraulic cylinders. The swing function is powered by a hydraulic motor and incorporates an anti-shock valve, two pairs of check valves, one pair with anti-cavitation and the other with shuttle functionality, and the swing brake actuator. This brake engages when no motion is required, functioning as a holding device to secure the cabin.

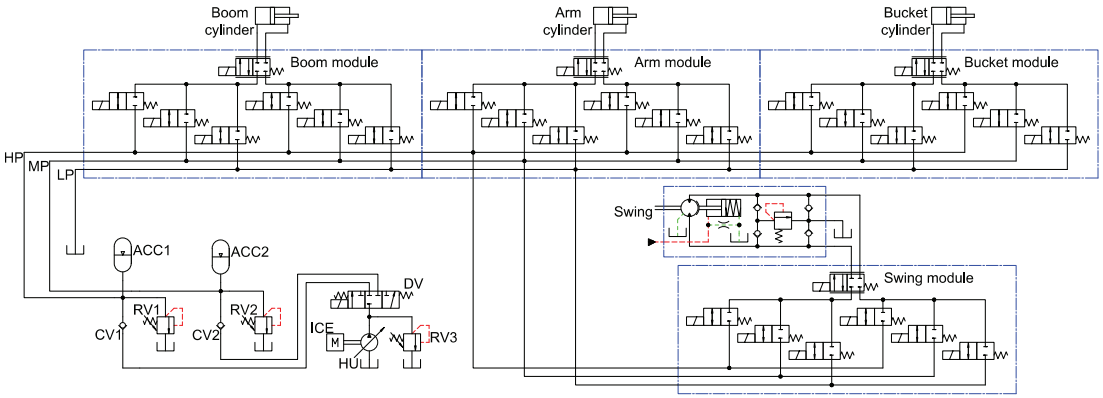


Figure 3. Simplified ISO scheme of the common pressure rail hydraulic circuit.

3.2 Simulation model

Figure 4 illustrates the simulation model of the proposed system in Simcenter Amesim. The subsystems in common with the original LS model are the ICE, the arm kinematic submodel, the linear actuators for boom, arm and bucket, and the cabin swing submodel. The ICE model is constituted by a variable-speed prime mover to enable analysis of a down-speeding solution, which is expected to yield greater improvements in fuel consumption compared to the LS approach.

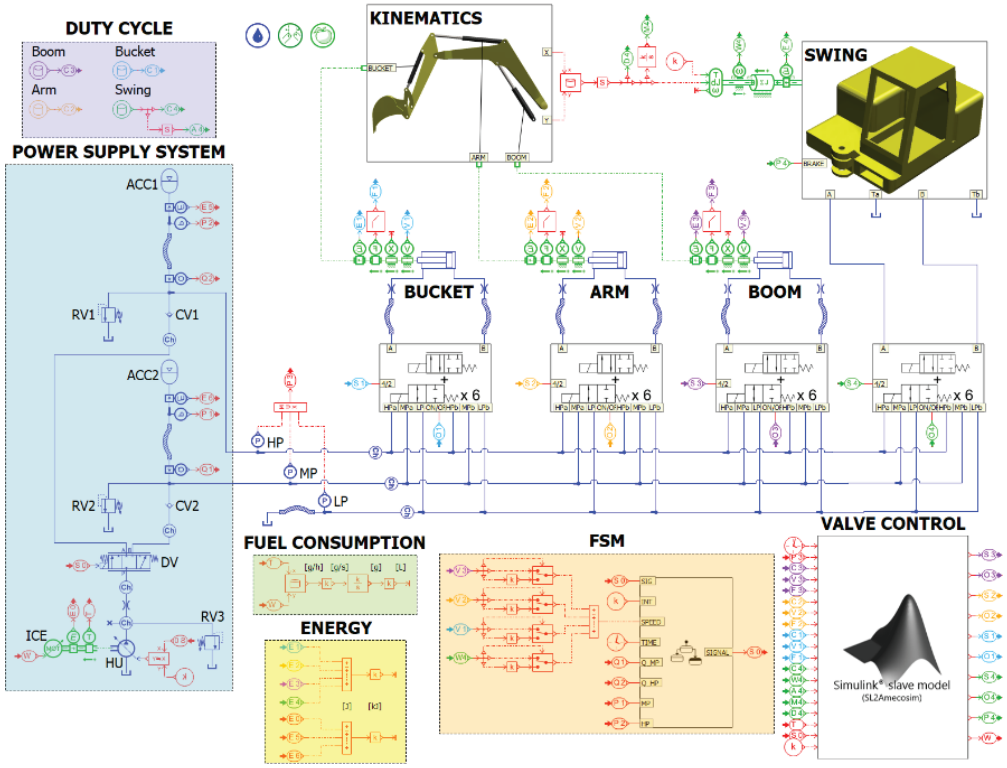


Figure 4. Complete simulation model of the common pressure rail excavator in Simcenter Amesim.

HU incorporates tabulated volumetric and mechanical-hydraulic efficiencies based on a similar unit as previuous described. The three relief valves are modeled with cracking pressures aligned with the maximum allowable pressures of the corresponding hydraulic lines and the pump outlet. The flow rate-pressure gradients are set to realistic values to reflect typical operating conditions. The directional valve (DV) was designed using the Valve Builder Tool to regulate flow from the pump. It was configured for a nominal flow rate of 200 L/min and a nominal pressure drop of 2 bar. The accumulators (ACC1 and ACC2) are sized and precharged to minimize throttling losses caused by imperfectly matched operating modes and external loads. The key parameters for these devices are listed in Table 1. Here, “allowable” refers to the pressure thresholds used by the controller to manage accumulator charging (with the control logic detailed in the next section), while with “minimum” and “maximum” denote the actual pressure specifications of the accumulator, used for selecting suitable devices on the market.

Table 1. HP and MP accumulator parameters.

Parameter	HP	MP	Unit
Max Allowable Pressure ($p_{th,max}$)	175	85	bar
Min Allowable Pressure ($p_{th,min}$)	140	60	bar
Max Pressure (p_2)	270	120	bar
Min Pressure (p_1)	100	44	bar
Gas Pre-Charge Pressure (p_0)	90	40	bar
Nominal Volume (V_0)	30	30	L

The six on/off valves for mode switching and the four-port two-position proportional valve for flow regulation are enclosed within a supercomponent, connecting the individual actuation systems to the common pressure lines. An internal view of the valve modules is shown in Fig. 5. The characteristic flow rate at maximum opening, along with the corresponding pressure drop, was defined based on commonly used valves in similar applications. Furthermore, the selection of all valves within the new architecture is based on appropriately sized components, determined according to the expected volumetric flow rates of the specific application.

References for the supercomponent structure of the arm kinematics and the cabin swing can be found respectively in references [6] and [11].

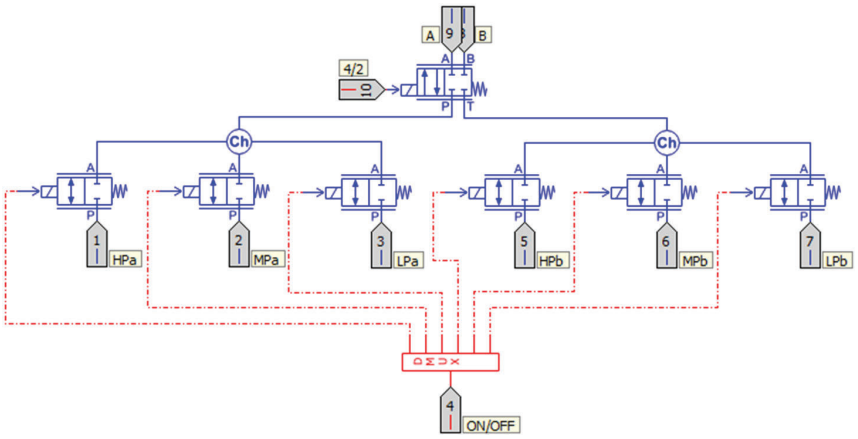


Figure 5. Internal view of the valve module supercomponent in Simcenter Amesim.

3.3 Control logic

The controller performs two main functions: selecting the appropriate pressure lines (via on/off valves) for the actuator chambers and cabin motor based on external forces, torques, and required speeds, and modulating the proportional valves to match actuator speeds with joystick outputs. Developed in Simulink and executed in Amesim via co-simulation, the controller leverages synchronized solvers from both environments. It is important to note that the control logic used in these key simulations, designed to assess system performance in terms of fuel consumption

and energy management, is not intended as the final implementation for the actual application. For instance, in this setup, the controller relies on actual forces applied at the actuators rather than pressure signals from the cylinder chambers, which are typically used in practical applications. Nevertheless, the primary objective of this control logic is to accurately replicate the working cycles of the baseline system to assess the hydraulic system performance, rather than to analyse the control strategy itself.

Analysing the interaction between the baseline LS excavator and its environment is essential, particularly the forces during the dig-and-dump cycle, which inform the CPR control strategy. To ensure signal accuracy, low-pass filters are applied to sensor data, reducing high-frequency noise. This prevents signal distortion and control instability, enabling reliable force trend identification for the boom, arm, and bucket. To optimize system efficiency and fully utilize the energy stored in the accumulators, a dedicated control logic for pump displacement was developed. The pump operates only when necessary and always at maximum displacement, reducing energy waste and ensuring required flow is delivered when needed.

Each accumulator is equipped with both a pressure sensor and a flow sensor, providing essential data for the accumulator charging controller. The control strategy was implemented using Amesim State Chart tool, which supports the development of finite state machines (FSMs). The system operates through a set of defined states, each triggered by specific conditions:

- Standby: the pump remains inactive when accumulator pressures are above a lower threshold and there is no immediate flow demand.
- Pump Charging HP Accumulator: the pump enters this state when the HP accumulator pressure falls below its lower threshold, initiating charging.
- Pump Charging MP Accumulator: if the MP accumulator pressure drops below its threshold, and the HP accumulator does not require charging, the pump charges the MP accumulator, but the HP accumulator always has priority.

While this pressure-threshold-based strategy ensures the pump operates only when strictly necessary, it is more effective in duty cycles with low average power demand. In high-demand cycles, such as dig-and-dump operations, relying solely on pressure thresholds may cause the accumulator to empty before recharging begins. To prevent this, the system can incorporate real-time HP and MP flow demand data to trigger charging proactively, before pressure falls below the lower limit. A volumetric flow rate threshold can be defined to detect high actuator demand, prompting the system to charge the HP or MP accumulators accordingly. The output signal of the FSM is sent to the directional valve (DV), which regulates the spool position and connects the pump to the appropriate pressure line. Additionally, it controls the pump, switching its state between zero displacement and full displacement as needed.

Moreover, the configuration of the on/off valve openings for the actuators is determined by identifying the optimal pressure combination that can counteract the external forces. Specifically, this involves minimizing the difference between the actuator exerted force, evaluated across all possible pressure combinations in the piston and rod chambers, and the external force, with the computation adjusted according to whether the actuator is in extension or retraction. The resulting optimal pressures indicate the necessary switching states of the six on/off valves. A similar approach is used for the hydraulic motor driving the cabin swing, aiming to achieve torque control instead of force control.

4. Duty cycles

To ensure a fair evaluation of the CPR system performance relative to the LS system, it is crucial to define duty cycles that accurately assess the full potential of each architecture while reflecting real-world operating conditions of the vehicle. Specifically, the dig-and-dump and levelling cycles represent the majority of the excavator operational activity. The following section provides a detailed description of these test cycles.

4.1 Dig-and-dump

The dig-and-dump cycle, illustrated in Fig. 6a, follows the JCMAS standard [14] and consists of the following steps, where positions A to E correspond to different excavator phases:

1. Approach to the Site (A): the excavator approaches the excavation point with its arm fully extended and actuators retracted, positioning itself for material extraction.
2. Penetration and Lifting (B): the bucket penetrates the material to be excavated. Once the material is secured, the arm lifts the bucket by combining arm extension and bucket lifting, ensuring a firm grip on the load.
3. Rotation (C): the excavator arm and bucket rotate 110° to position the material over the discharge point.
4. Dumping (D): once positioned, the bucket tilts to release the material.
5. Return to the Starting Position (E): the excavator repositions itself for the next cycle. The arm fully extends, and the bucket returns to its initial position, ready for the next load.

Fig. 6b illustrates the displacement of the linear actuators and the cabin swing motion as a function of time.

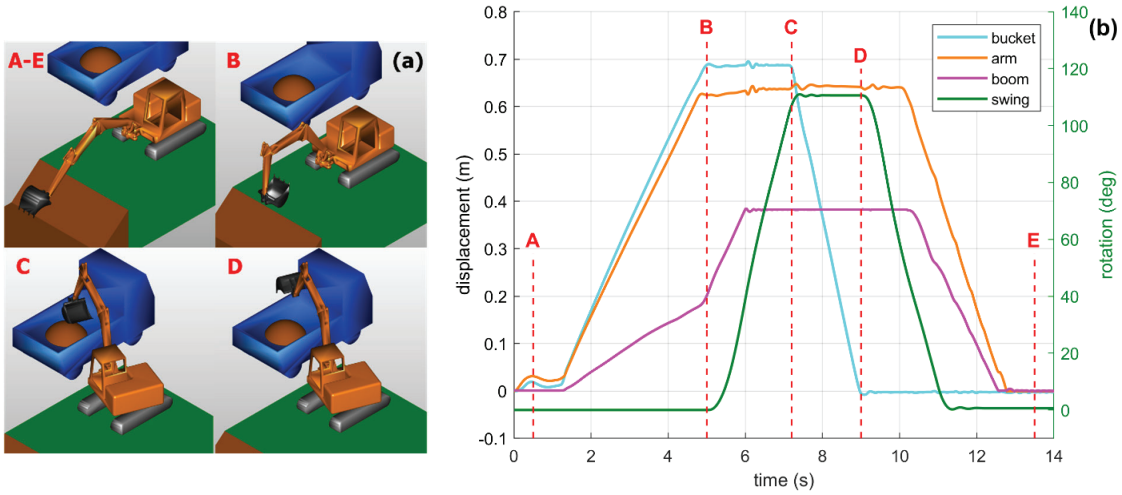


Figure 6. (a) 3D rendering of the relevant excavator positions in the dig-and-dump cycle; (b) simulated displacement of the actuators in the dig-and-dump cycle.

Notably, when swing rotation is activated, the boom speed increases, as indicated by the increased slope of the magenta curve after B point. In the reference hydraulic system, this effect results from the activation of the flow boost valve (VB), whereas in the CPR system, it is achieved by adjusting the spool position of the four-port two-position directional control valve associated with the boom actuator.

In the CPR model, joystick input commands from the cabin are supplied to directional, proportional control valves, ensuring that actuator movements precisely match those in the reference system. In particular, the joysticks are actuated fully to the end of their stroke, without modulation. As a result, the directional control valves operate with the spools fully shifted to one extreme or the other. This approach allows for a comparison under identical useful mechanical energy conditions.

4.2 Levelling

The levelling cycle simulates a different excavator operation than the dig-and-dump cycle, providing a broader evaluation of both system architectures. Testing both cycles helps determine whether performance advantages observed in one task apply across different applications.

Energy efficiency in a levelling operation, which demands continuous and controlled movement, can vary significantly from cycles involving more intense lifting and material transport. Leveling, in particular, requires a high degree of precision and control, making this test essential for evaluating both the accuracy of the control system and the excavator ability to maintain a constant angle and uniform depth. In this scenario, the joysticks are no longer actuated to the end of their stroke; instead, they are finely adjusted to achieve the required precision in angle and depth control.

The cycle consists of two main phases:

1. Levelling: the bucket moves along the ground surface at a constant angle, removing irregularities while the arm and boom control depth and angle of leveling.
2. Return to Start: after completing a leveling pass, the arm and boom return to the starting position to begin the new cycle.

Figure 7a highlights two key positions in the levelling cycle, labeled A and B, while Fig. 7b illustrates the displacement of the linear actuators over time.

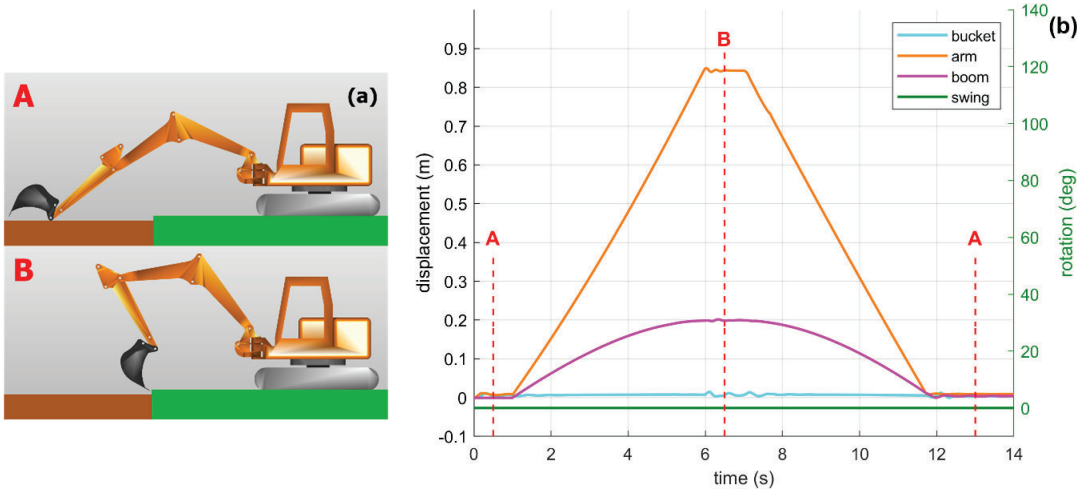


Figure 7. (a) 3D rendering of the relevant excavator positions in the levelling cycle; (b) simulated displacement of the actuators in the levelling cycle.

5. Results

5.1 Displacement comparison in dig-and-dump cycle: LS vs. CPR

The CPR architecture is initially compared with the LS architecture by analysing the displacement of the actuators during the dig-and-dump cycle. This comparison allows for a fair evaluation of the mechanical energy supplied by the engine and the fuel consumption, while ensuring that the same useful mechanical energy is delivered to the actuators in both models.

Figure 8 illustrates the displacement of the bucket (a), arm (b), and boom (c) linear actuators, along with the rotation of the cabin swing (d). The comparison is shown between the CPR model (dashed, blue line) and the LS model (solid, red line).

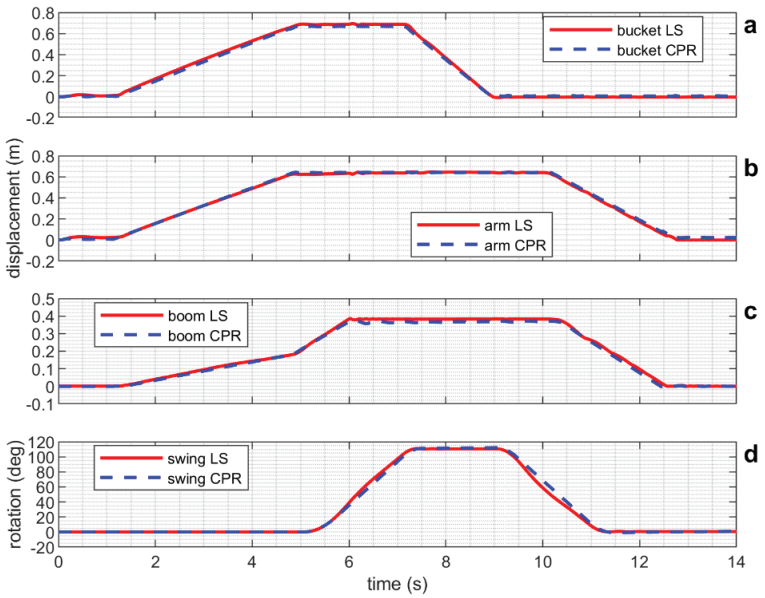


Figure 8. Bucket (a), arm (b) and boom (c) displacement, and swing rotation (d) comparison for CPR and LS architectures during the dig-and-dump cycle.

For the first three plots (a, b, and c), which show the displacement of the linear actuators, the curves for both the CPR and LS models are closely aligned, indicating a strong correspondence between the two sets of data. The maximum observed discrepancies are 3.5 cm for the bucket actuator (≈5.0% of maximum extension), 2.8 cm for the arm actuator (≈4.4%), and 2.5 cm for the boom actuator (≈6.6%). In the final plot (d), which illustrates the rotation of the cabin swing, the two models follow a similar trend; however, some discrepancies are noticeable during motion, with a maximum difference of 9.9 degrees (≈8.9% of maximum rotation). It is worth noting that in the CPR model, the cabin rotates by the required angle and then is reset to its initial position, ensuring that both the start and final conditions of the cycle are the same as in the LS architecture. The slight differences in motion profiles may be attributed to small errors in the opening signal of the proportional directional control valve, which regulates the actuator speeds.

5.2 Comparison between LS and CPR at same engine speed

To enable a fair comparison between the LS and CPR architectures, the internal combustion engine was operated at a constant speed of approximately 2400 rpm in both cases. According to the simulation results presented in Tables 2 and 3, the mechanical energy delivered to the

actuators over a complete working cycle remains virtually unchanged between the two systems. This confirms that the working performance of the excavator is preserved despite the different hydraulic control strategies.

Table 2 summarizes the results for the dig-and-dump cycle, including mechanical energy at the internal combustion engine shaft, net mechanical energy at the actuators, and fuel consumption. While delivering nearly the same mechanical energy to the actuators, the CPR architecture operates more efficiently and consumes less fuel compared to the LS system. Specifically, the percentage of actuator net energy relative to the engine shaft energy is 16.4% for the LS system and 30.9% for the CPR system. This improved efficiency is primarily due to reduced valve group losses, as the prime mover and actuator operations remain identical in both architectures. Moreover, the CPR system achieves a 33.7% reduction in fuel consumption compared to the LS architecture.

Table 2. Input and output energy and fuel consumption for LS and CPR architectures during the dig-and-dump cycle assuming constant ICE speed.

	LS	CPR	Reduction [%]
ICE shaft mechanical energy [kJ]	382.9	210.8	44.9
Actuator net mechanical energy [kJ]	62.7	65.2	—
Fuel consumption [g]	27.9	18.5	33.7

To further highlight the improved performance of the CPR architecture and validate the model across a broader range of operating conditions, Table 3 presents the same set of results as Table 2, but for the levelling cycle. Although the thermal efficiency of the engine is reduced in this cycle, due to operation at lower torques and in less efficient regions of the engine map, as only the medium-pressure rail is utilized, the CPR architecture still demonstrates an advantage over the LS system. In this scenario, hydraulic losses from the on/off valve block and accumulators have a reduced impact, while losses associated with proportional valves become more significant.

Table 3. Input and output energy and fuel consumption for LS and CPR architectures during the levelling cycle assuming constant ICE speed.

	LS	CPR	Reduction [%]
ICE shaft mechanical energy [kJ]	226.2	95.3	57.9
Actuator net mechanical energy [kJ]	15.6	16.2	—
Fuel consumption [g]	19.4	12.7	34.5

The primary benefit of the CPR architecture lies in its ability to minimize throttling by selecting the appropriate operating mode based on the actuator demands. However, this advantage is less evident here, as the actuator pressure requirements remain relatively constant.

As a result, the system tends to operate in a single mode, adjusting pressure through throttling rather than mode switching. Additionally, the percentage of recoverable energy in this cycle is lower compared to the dig-and-dump cycle. This is expected, given the absence of significant dynamic loads and the lack of kinetic energy recovery from cabin movement, as the cabin remains stationary throughout the levelling cycle. In this second cycle, the percentage of actuator net energy relative to the engine shaft energy is 6.9% for the LS system and 17.0% for the CPR system. Moreover, the CPR system achieves a 34.5% reduction in fuel consumption compared to the LS architecture.

5.3 Effects of engine down-speeding

By decoupling the energy supplied by the power system from the energy demanded by the actuators, the CPR architecture enables strategies to enhance thermal engine efficiency. One such strategy is down-speeding, which shifts the engine operating points to lower speeds and higher torques, aligning with its most efficient range. In this case, engine speed is reduced to around 1200 rpm during active operation and further lowered to an idle speed of 800 rpm whenever accumulator charging is not required, thus avoiding the need for constant-speed operation throughout the entire duty cycle.

Table 4 presents the same set of results as in the previous section, but for the CPR architecture using the down-speeding strategy, applied to both the dig-and-dump and levelling cycles. As shown in Table 4, the down-speeding strategy leads to a further reduction in the mechanical energy required at the ICE shaft, with a corresponding decrease in fuel consumption. Notably, the ratio of actuator energy to engine shaft energy improves from 30.9% to 33.6% for the dig-and-dump cycle, and from 17.0% to 18.2% for the levelling cycle. A similar trend is observed in the fuel consumption reduction, which improves from 33.7% to 58.8% in the dig-and-dump cycle, and from 34.5% to 68.0% in the levelling cycle.

Table 4. Input and output energy and fuel consumption for CPR architecture during the dig-and-dump and levelling cycles considering engine down-speeding.

	Dig-and-dump	Levelling	Reduction [%]	
			Dig-and-dump	Levelling
ICE shaft mechanical energy [kJ]	192.7	89.0	49.7	60.6
Actuator net mechanical energy [kJ]	64.7	16.2	—	—
Fuel consumption [g]	11.5	6.2	58.8	68.0

6. Conclusion

This study compared the Load Sensing and Common Pressure Rail hydraulic architectures for a 9-ton excavator under two typical duty cycles (dig-and-dump and levelling). The results clearly demonstrate the superior efficiency of the CPR system in terms of reduced mechanical energy demand at the internal combustion engine shaft and lower fuel consumption. By decoupling actuator demand from power generation, the CPR architecture enables more efficient operation strategies, such as down-speeding. This strategy further improved overall efficiency, with actuator-to-engine energy ratios increasing and fuel consumption significantly reduced.

Considering a very common duty cycle for this type of machines, the CPR system saved 33.7% of the fuel used by the LS system, and this improvement increased to 58.8% with the down-speeding strategy. These findings confirm the CPR architecture potential for improving energy efficiency and reducing environmental impact in mobile hydraulic systems. Future work may explore how the proposed architecture performs under more demanding duty cycles, such as overcoming obstacles that require operation at higher pressure levels. In these scenarios, the accumulator pressure may fall short of meeting the actuator load demands. Furthermore, CPR architectures exhibit limitations when operating near the system maximum pressure. For excavators larger than the one studied in this work, relying on a single pump (even one with increased displacement) and only two accumulators may not be adequate. Therefore, future research could investigate new architectures based on the CPR concept to address the challenges of operating at maximum pressure and to better adapt the system for larger-scale excavators. Additionally, the development of an advanced control logic for actuator management and accumulator charging represents another important direction for future work.

References

[1] Casoli, P., Zardin, B., Ardizio, S., Borghi, M., Pintore, F., Mesturini, D., The Hydraulic Power Generation and Transmission on Agricultural Tractors: feasible architectures to reduce dissipation and fuel consumption–Part 2, E3S Web of Conferences, 197, 07010, 2020. DOI: 10.1051/e3sconf/202019707010.
[2] Bonavolontà, A., Dolcin, C., Marani, P., Frosina, E., Senatore, A., Comparison of energy saving and recovery systems for hydraulic mobile machines, AIP Conference Proceedings, 2191, 020025, 2019. DOI: 10.1063/1.5138758.
[3] Fassbender, D., Brach, C., Minav, T., Energy-efficiency comparison of different implement powertrain concepts to each other and between different heavy-duty mobile machines, International Journal of Fluid Power, 25 (2), 127-144, 2024. DOI: 10.13052/ijfp1439-9776.2521.
[4] Tian, X., Guo, X., Stump, P., Dessy, G., Vacca, A., Fiorati, S., Pintore, F., New Hydraulic Control Technologies for Improving the Energy Efficiency of the Hydraulic System of Agricultural Tractors and Their Implements, International Journal of Fluid Power, 25 (2), 203-224, 2024. DOI: 10.13052/ijfp1439-9776.2525.
[5] Casoli, P., Scolari, F., Minav, T., Rundo, M., Comparative energy analysis of a load sensing system and a zonal hydraulics for a 9-tonne excavator, Actuators, 9(2), 39, 2020. DOI: 10.3390/act9020039.
[6] Fresia, P., Rundo, M., Padovani, D., Altare, G., Combined speed control and centralized power supply for hybrid energy-efficient mobile hydraulics, Automation in Construction, 140, 104337, 2022. DOI: 10.1016/j.autcon.2022.104337.
[7] Schmidt, L., van Binsbergen-Galán, M., Knöll, R., Riedmann, M., Schneider, B., Heemskerk, E., Energy Efficient Excavator Implement by Electro-Hydraulic/Mechanical Drive Network, International Journal of Fluid Power 25(4), 413-438, 2024. DOI: 10.13052/ijfp1439-9776.2541.
[8] Padovani, D., Adding Damping to Energy-Efficient Electro-Hydraulic Drives Using Observed Pressure, 2025 Australian & New Zealand Control Conference (ANZCC), IEEE, Gold Coast, Australia, 2025. DOI: 10.1109/ANZCC65042.2025.10873347.
[9] Zhang, Q., Kong, X., Yu, B., Ba, K., Jin, Z., Kang, Y., Review and development trend of digital hydraulic technology, Applied Sciences, 10(2), 579, 2020. DOI: 10.3390/app10020579.
[10] Sciatti, F., Tamburrano, P., Distaso, E., Amirante, R., Digital hydraulic valves: Advancements in research, Heliyon, 10(5), e27264, 2024. DOI: 10.1016/j.heliyon.2024.e27264.
[11] Altare, G., Padovani, D., Nervegna, N., A commercial excavator: Analysis, modelling and simulation of the hydraulic circuit, SAE Technical Paper No. 2012-01-2040, 2012. DOI: 10.4271/2012-01-2040.
[12] Vukovic, M., Leifeld, R., Murrenhoff, H., Reducing fuel consumption in hydraulic excavators—A comprehensive analysis, Energies 10(5), 687, 2017. DOI: 10.3390/en10050687.
[13] Vukovic, D. I. M., Leifeld, M. S. R., Murrenhoff, I. H., STEAM–a hydraulic hybrid architecture for excavators, 10th International Fluid Power Conference, Dresden, Germany, 2016. DOI: 10.1007/s41321-016-0523-9.
[14] Earth-Moving Machinery—Fuel Consumption on Hydraulic Excavator—Test Procedure, JCMAS H020:2007, Tokyo, Japan, 2007.